This paper is published as part of a *Dalton Transactions* themed issue on:

Metal-catalysed Polymerisation

Guest Editors: Barbara Milani and Carmen Claver
University of Trieste, Italy and Universitat Rovira i Virgili, Tarragona, Spain

Published in issue 41, 2009 of *Dalton Transactions*

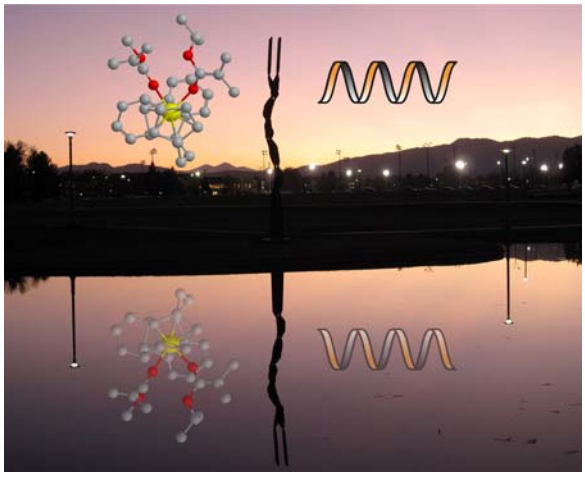

Image reproduced with permission of Eugene Chen

Articles published in this issue include:

PERSPECTIVES:

HOT PAPERS:

Visit the *Dalton Transactions* website for more cutting-edge organometallic and catalysis research
www.rsc.org/dalton

Vanadium-based imido-alkoxide pro-catalysts bearing bisphenolate ligands for ethylene and ε-caprolactone polymerisation†

Abdessamad Arbaoui,[a] Carl Redshaw,*[a] Damien M. Homden,[a] Joseph A. Wright[a] and Mark R. J. Elsegood[b]

Received 4th February 2009, Accepted 15th May 2009
First published as an Advance Article on the web 7th July 2009
DOI: 10.1039/b902402f

The pro-catalysts [V(NAr)(L)(OR)] (Ar = *p*-tolyl, *p*-ClC_6H_4, *p*-$(OMe)C_6H_4$, *p*-$(CF_3)C_6H_4$; R = *t*-Bu, *i*-Pr, *n*-Pr, Et, $C(CH_3)(CF_3)_2$) have been prepared in good yields from the reaction of [V(NAr)$(OR)_3$] and the bisphenol 2,2′-CH_3CH[4,6-(*t*-Bu)$_2C_6H_2OH]_2$ (LH_2). X-Ray crystal structure determinations for the Ar = *p*-tolyl, R = *t*-Bu (**1**), R = $C(CH_3)(CF_3)_2$ (**2**) and Ar = *p*-ClC_6H_4, R = *t*-Bu (**3**) derivatives revealed monomeric complexes, whereas use of R = *i*-Pr, *n*-Pr or Et led to alkoxide-bridged dimeric structures of the form [V(NAr)(L)(μ-OR)]$_2$ (R = *i*-Pr, Ar = *p*-tolyl (**4**), *p*-ClC_6H_4 (**5**), *p*-$(CF_3)C_6H_4$ (**6**), *p*-$(OMe)C_6H_4$ (**7**); R = *n*-Pr, Ar = *p*-tolyl (**8**), *p*-$(CF_3)C_6H_4$ (**9**); R = Et, Ar = *p*-ClC_6H_4 (**10**), *p*-tolyl (**11**)). Complexes **1–11** yield highly active ethylene polymerisation catalysts when treated with DMAC (dimethylaluminium chloride) in the presence of ETA (ethyltrichloroacetate), with activities in the range 38 800 to 75 200 g $mmol^{-1}$ h^{-1} bar^{-1}. The molecular weights of the resultant polymers were in the range 37 000 to 411 000 g mol^{-1}, with molecular weight distribution 2.2 to 4.7. The effect of the nature of the *para*-arylimido substituent and the alkoxide group OR upon the catalytic activity has been investigated. For ε-caprolactone polymerisation, mononuclear **1–3** exhibit low conversion (≤25%; 0% for **2**), whereas use of the dimeric species **4–11** led to higher conversions (41–78%).

Introduction

Given the success of a number of investigators when examining group IV metal chelating aryloxide systems for polymerisation processes,[1] we have subsequently screened a number of group V metal di- and triphenolate pro-catalysts. In the case of niobium and tantalum, catalytic results were poor and such studies were discontinued.[2] However, a number of vanadyl complexes bearing chelating aryloxide ligands exhibited extremely high catalytic activities (*ca.* 100 000 g $mmol^{-1}$ h^{-1} bar^{-1}) and, in the preceding paper, we extended this family to include –S– and $–SO_2–$ bridged chelating aryloxides.[3] The exact nature of the active species is still unknown, though it is thought to involve vanadium in the +3 state.[4] Amongst this group of aryloxide pro-catalysts were a new family of dimeric vanadyl complexes bearing bisphenolate ligands of the type 2,2′-CHR[4,6-(*t*-Bu)$_2C_6H_2OH]_2$ (R = H, Me (LH_2)), and possessing the structure **I** (Chart 1). We were interested in how the electronic and steric factors associated with this type of pro-catalyst structure might affect the catalytic activity/control of the ethylene polymerization process. Given that the oxo group is isoelectronic with the organoimido group, it was of interest to investigate the related organoimido containing species. We note that recent reports by Moriuchi and Hirao have shown how the imido group geometrical parameters can be controlled by the *para* substituent of the aryl moiety (π-conjugation rather than inductive effects) in a series of vanadium(v) complexes.[5] We also note that in the patent literature there is mention of [V(NAr)(bisphenolate)Cl]-type pro-catalysts for olefin co-polymerisation and terpolymerisation with other dienes, where a number of imido groups were employed possessing a variety of electron-withdrawing groups, for example 2,4,6-$Cl_3C_6H_2N$.[6]

Herein, we report our investigations using the readily available vanadium precursors [V(NAr)$(OR)_3$] (Ar = *p*-tolyl, *p*-ClC_6H_4, *p*-$(OMe)C_6H_4$, *p*-$(CF_3)C_6H_4$; R = *t*-Bu, $C(CH_3)(CF_3)_2$, *i*-Pr, *n*-Pr, Et),[7] and their interaction with the chelating bisphenol 2,

[a]*Energy Materials Laboratory, School of Chemical Sciences and Pharmacy, University of East Anglia, Norwich, UK NR4 7TJ. E-mail: carl.redshaw@uea.ac.uk*
[b]*Chemistry Department, Loughborough University Loughborough, Leicestershire, UK LE11 3TU*

† Electronic supplementary information (ESI) available: Selected polymerisation data, X-ray crystallographic files in CIF format for the structure determinations of compound **1–10**. CCDC reference numbers 718351–718360. For ESI and crystallographic data in CIF or other electronic format see DOI: 10.1039/b902402f

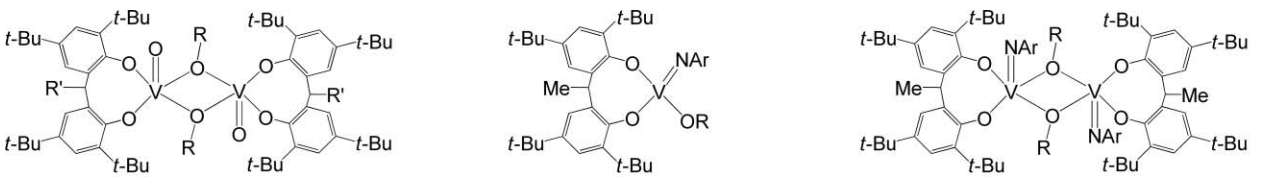

I (R = *n*-Pr, R' = H, Me)

II (Ar = *p*-tolyl, *p*-ClC_6H_4; R = *t*-Bu, $C(CF_3)_2Me$)

III (Ar = *p*-tolyl, *p*-ClC_6H_4, *p*-$(MeO)C_6H_4$, *p*-$CF_3C_6H_4$; R = *i*-Pr, *n*-Pr, Et)

Chart 1 Pro-catalysts [V(O)(L)(μ-OR)]$_2$ (**I**), [V(NAr)(L)(OR)] (**II**) and [V(NAr)(L)(μ-OR)]$_2$ (**III**).

2′-ethylidene-bis(4,6-di-*tert*-butylphenol), which affords products possessing one of two classes of structure (see **II** and **III**, Chart 1) depending on the steric hindrance associated with the alkoxide group R. The ability of the complexes to act as pro-catalysts for ethylene polymerisation has been investigated and, given the presence of the alkoxide ligand, we have also assessed their ability to polymerise ε-caprolactone. Chelating bisphenols such as LH_2 have been employed previously as ancillary ligands in catalytic systems for the ring opening of lactones and lactides, primarily in conjunction with aluminium, zinc, titanium and lanthanide centres.[8]

Results and discussion

General

Interaction of the arylimido-trialkoxides $[V(NAr)(OR)_3]$ with one equivalent of the bisphenol LH_2 in refluxing toluene afforded, following work-up, complexes of the form $[V(NAr)(L)(OR)]_n$ (n = 1 or 2) as orange-red crystalline solids in moderate to high yield (*ca.* 40–80%). Washing with cold acetonitrile removed any minor vanadyl species of the form $[V(O)(L)(OR)]_n$ (n = 1 or 2), leaving the analytically pure imido complex on the frit. Stoichiometrically such complexes are formed *via* the loss of two molecules of alcohol per vanadium centre.

Monomeric *tert*-butoxides

In the case of the *tert*-butoxides (Ar = *p*-tolyl, R = *t*-Bu (**1**) and $C(CH_3)(CF_3)_2$ (**2**); Ar = *p*-(Cl)C_6H_4, R = *t*-Bu (**3**)), prisms suitable for single-crystal X-ray structure determinations were grown from saturated acetonitrile solutions on prolonged standing at ambient temperature. The molecular structures are shown in Fig. 1 with selected bond lengths and angles given in Table 1; crystallographic data are presented in Table 10. The *tert*-butoxide complexes obtained are all monomeric. The geometry about the vanadium centre in **1–3** is *pseudo* tetrahedral with angles varying from ideal in the ranges 105.15(5) to 113.39(9)° for **1**, 103.81(6) to 114.00(5)° for **2**, and 105.72(11) to 115.61(12)° for **3**. The organomido groups in each complex can be considered linear (V(1)–N(1)–C(5) = 175.73(17)° (**1**), 175.63(13)° (**2**) and 176.2(2)° (**3**)).[9] The V–N bond lengths (1.657(2) (**1**), 1.6487(15) (**2**) and 1.653(3) Å (**3**)) are in the range of values reported for related arylimido vanadium(V) complexes (1.644(3) to 1.678(3) Å).[5,7,9,10] In all of the *tert*-butoxide

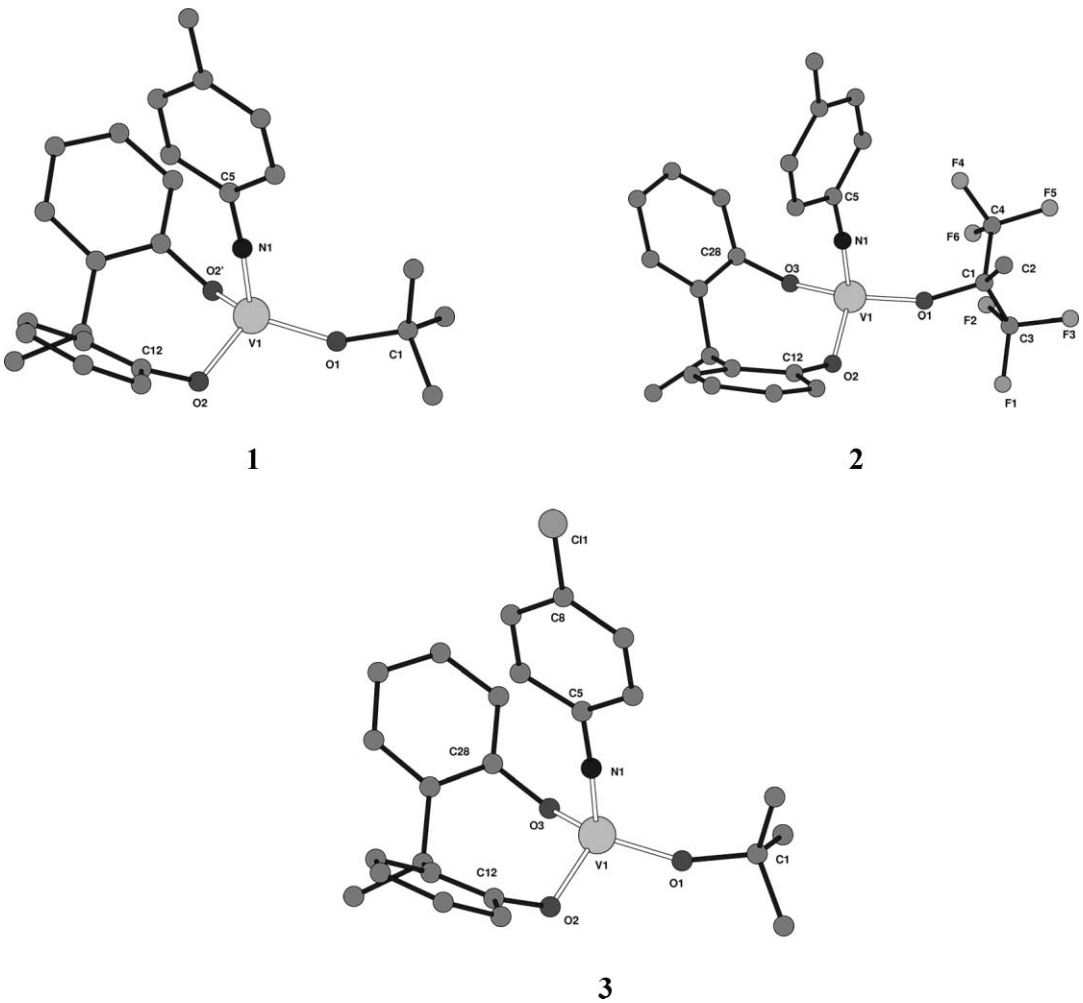

Fig. 1 CAMERON representation of the structures of **1**, **2** and **3** showing spheres of arbitrary size; hydrogen atoms and *t*-Bu groups on the phenolates have been omitted for clarity.

Table 1 Selected bond lengths (Å) and angles (°) for **1**, **2** and **3**

	1	**2**	**3**
Bond lengths/Å			
V(1)–N(1)	1.657(2)	1.6487(15)	1.653(3)
V(1)–O(1)	1.7509(15)	1.8001(11)	1.738(2)
V(1)–$O_{phenolate}$	1.8118(11)	1.7966(12) and 1.8097(12)	1.802(2) and 1.804(2)
Bond angles/°			
N(1)–V(1)–O(1)	113.39(9)	112.94(7)	115.61(12)
N(1)–V(1)–$O_{phenolate}$	105.15(5)	105.45(7) and 103.81(6)	105.72(11) and 105.92(12)
O(1)–V(1)–$O_{phenolate}$	112.44(4)	111.23(7) and 114.00(5)	110.38(11) and 110.67(10)
V(1)–$O_{phenolate}$–$C_{phenolate}$	123.90(9)	120.68(10) and 131.04(10)	124.22(18) and 124.83(18)
V(1)–O(1)–C(1)	147.73(14)	146.77(12)	151.9(2)
V(1)–N(1)–C(5)	175.73(17)	175.63(13)	176.2(2)

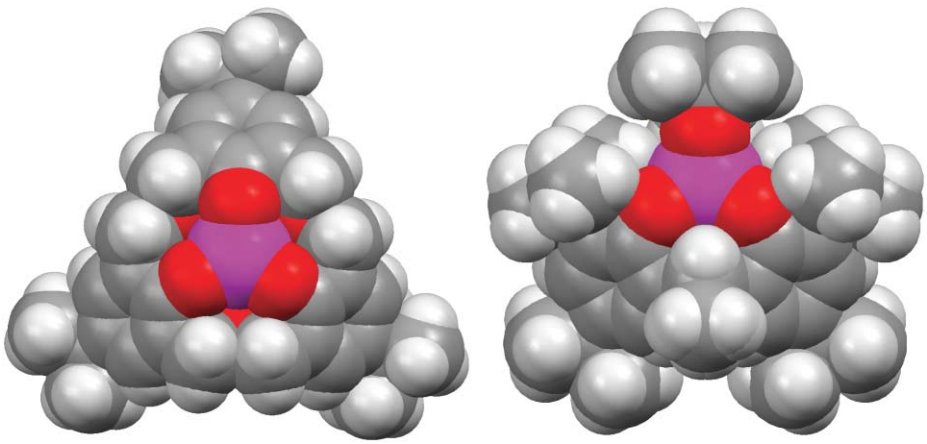

Fig. 2 Space filling diagrams of (left) [V(N*p*-tolyl)(hexahomotrioxacalix[3]arene)]$_2$ (only half of dimer shown) and (right) **1**.

complexes, the eight membered chelate rings adopt a flattened chair conformation, in contrast to the reported flattened boat conformation for the related chloro vanadium(v) oxo complex bearing the bisphenol ligand 2,2′-CH_2(4-Me-6-*t*-Bu$C_6H_2OH)_2$.[11] The V–O distances to the bisphenolate ligand (1.7966(12) to 1.8118(11) Å) are typical of those previously observed for vanadium(v) aryloxides (1.734(3) to 1.850(7) Å).[11,12] The V–O distances to the alkoxides are 1.7509(15) Å in **1**, 1.8001(11) Å in **2** and 1.738(2) Å in **3** and are somewhat shorter than those reported in other arylimido-alkoxy vanadium(v) complexes (1.842(1) to 1.888(3) Å).[3,5b,7] The alkoxo ligands adopt a bent arrangement (V(1)–O(1)–C(1) 147.73(14)° (**1**), 146.77(12) (**2**) and 151.9(2)° (**3**)).

We note that the coordination environment about the vanadium centre in complexes **1–3** shows a resemblance to the vanadium environment in the highly active hexahomotrioxacalix[3]arene-based vanadyl complexes as highlighted in Fig. 2.[13]

Dimeric structures/variation of imido substituent

When the R group in the precursor vanadium complex is less bulky than *tert*-butyl, an alkoxide-bridged dimeric structure is favoured. Given the recent observations of Moriuchi and Hirao,[5] we carried out single-crystal X-ray diffraction studies on a number of organoimido derivatives with various combinations of alkoxide group (OR) and arylimido group, in order that we might observe structure/activity relationships (*vide infra*). As an entry point, we chose the R = isopropoxy system [V(NAr)(O*i*-Pr)$_3$].[7b] For Ar = *p*-tolyl (**4**), *p*-ClC_6H_4 (**5**), *p*-$CF_3C_6H_4$ (**6**) and *p*-(OMe)C_6H_4 (**7**), samples suitable for single-crystal X-ray diffraction studies were grown from saturated solutions of acetonitrile at 0 °C. In all cases, [V(NAr)(μ-O*i*-Pr)L]$_2$ crystallizes as a centrosymmetric dimer (see Fig. 3a–d). Selected bond lengths and angles are collected in Table 2. The geometry at each vanadium is best described as trigonal bipyramidal, with N(1) and O(1′) occupying the apical sites; the Reedijk criteria calculated for **4–7** ($\tau \approx 0.8$) confirms the geometry assignment.[14] The three oxygen atoms O(1), O(2) and O(3) occupy the equatorial sites, with the vanadium centre located about 0.26 Å out of the mean plane of the three oxygen atoms in each case. As in **1–3**, the eight membered ring chelates in **4–7** adopt a flattened chair conformation, with O(2)–V(1)–O(3) bite angles in the range 109.68(7) to 112.19(6)°. These bite angles are close to that reported by Toscano *et al.* (106.9(2)°) for a related oxo vanadium(v) complex bearing a bisphenolate ligand.[11] The arylimido group is bound to the metal almost directly opposite the longer bridging isopropoxy group, and shows the anticipated geometry with near linear V(1)–N(1)–C(5) angles in the range 170.6(4)–173.3(3)°. The V(1)–N(1) distances do not differ significantly, and are all about 1.66 Å. In the case of **6**, the imido group shows disorder over two sets of positions. The major component (approx. 55% occupancy) has an angle at nitrogen

Table 2 Selected bond lengths and angles for **4–7**

	4	**5**	**6**	**7**
Bond lengths/Å				
V(1)–N(1)	1.662(3)	1.658(2)	1.651(3)	1.6566(17)
V(1)–O(1)	1.879(3)	1.8808(16)	1.880(2)	1.8632(12)
V(1)–O(2)	1.838(2)	1.8527(16)	1.821(2)	1.8373(13)
V(1)–O(3)	1.840(2)	1.8313(16)	1.821(2)	1.8295(12)
V(1)–O(1′)	2.205(2)	2.1838(16)	2.240(2)	2.2590(13)
V(1)···V(1′)	3.294	3.301	3.337	3.311
Bond angles/°				
N(1)–V(1)–O(1)	100.15(13)	102.34(8)	100.04(12)	101.15(7)
N(1)–V(1)–O(2)	98.25(13)	97.97(9)	97.49(11)	95.82(7)
N(1)–V(1)–O(3)	96.00(13)	97.15(8)	97.19(12)	98.51(7)
N(1)–V(1)–O(1′)	171.87(14)	173.97(8)	172.14(11)	174.32(6)
O(1)–V(1)–O(2)	120.33(10)	123.19(7)	121.51(10)	122.30(6)
O(1)–V(1)–O(3)	122.65(11)	119.40(7)	122.21(10)	118.96(6)
O(1)–V(1)–O(1′)	72.73(11)	71.63(7)	72.12(10)	73.54(6)
O(2)–V(1)–O(3)	110.98(11)	109.68(7)	110.06(10)	112.19(6)
V(1)–O(1)–V(1′)	107.27(11)	108.37(7)	107.88(10)	106.46(6)
V(1)–N(1)–C(5)	173.3(3)	172.54(17)	170.6(4) and 172.6(3)	171.47(15)

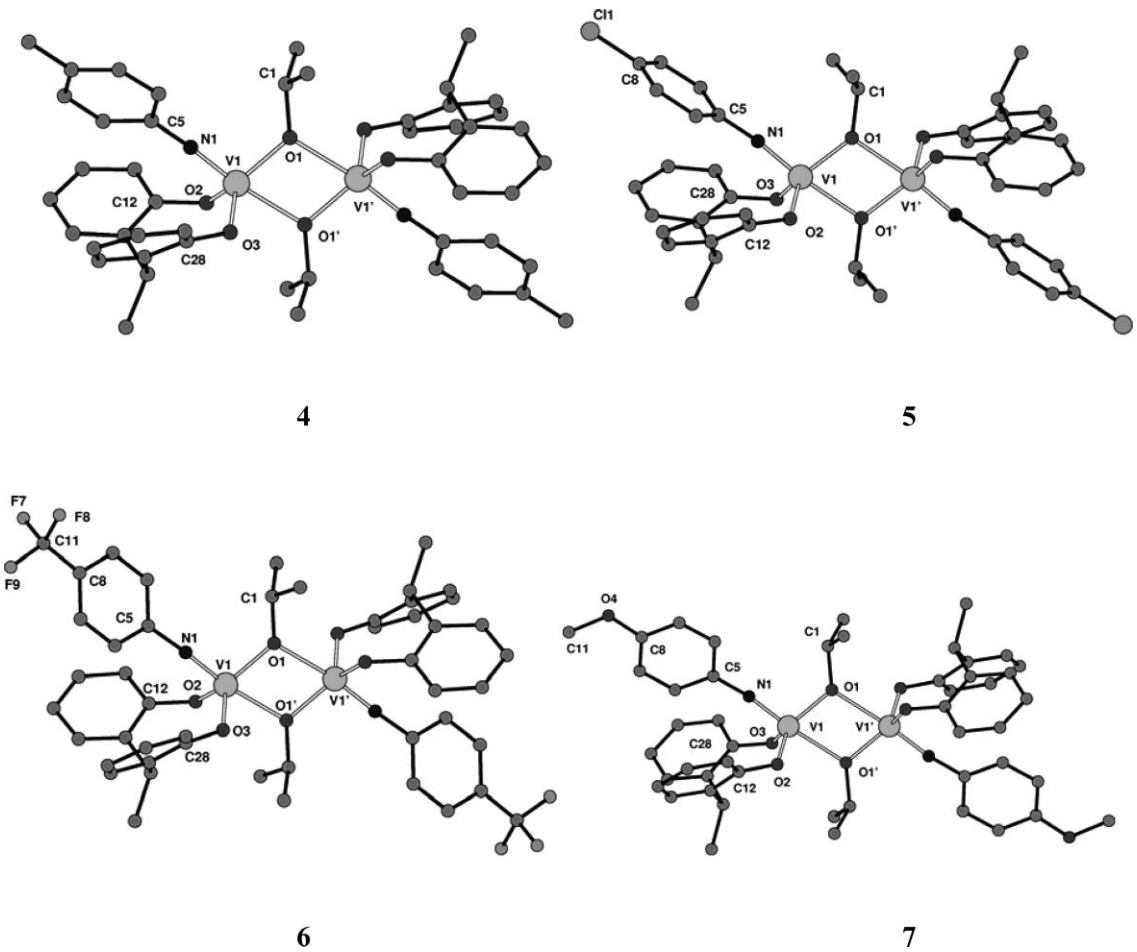

Fig. 3 CAMERON representation of the structures of **4**, **5**, **6** and **7** showing spheres of arbitrary size; hydrogen atoms and *t*-Bu groups on the phenolates have been omitted for clarity.

(C(34)–N(1)–V(1)) of 172.6(3)°, whereas the minor component shows an angle of 170.6(4)°. This disorder is carried through the whole imido ligand, with the entire aromatic ring and CF_3 group displaced. The two components are also rotated relative to one another, with the angle between normals to the mean planes of the aromatic rings being approximately 61°.

Variation of alkoxide group

Replacement of O*i*-Pr by the smaller O*n*-Pr or OEt groups leads to the formation of $[V(NAr)(\mu\text{-}OR)L]_2$, R = *n*-Pr, Ar = *p*-tolyl (**8**), *p*-$CF_3C_6H_4$, (**9**); R = Et, Ar = *p*-ClC_6H_4 (**10**), Ar = *p*-tolyl (**11**) (Fig. 4). Complexes **8–10** show the same general dimeric structure as the O*i*-Pr systems, although **10** is pseudo-symmetrical and lacks a crystallographic centre of symmetry. All three molecules crystallise with discrete solvent molecules in the cell: **8** crystallises with two CH_2Cl_2 per dimer, **10** with one CH_2Cl_2 per dimer and **9** with one CH_3CN per dimer. The geometric parameters, summarised in Table 3, show the similarity between these molecules and the O*i*-Pr analogues.

Spectroscopy

The ^{1}H NMR spectra of complexes **1–11** show little influence of the complexation on the chemical shift for the ethylidene CH(CH_3) grouping of the diphenol ligand. For example, in **5** and **6** this signal is shifted only *ca.* 0.1 ppm upfield compared with the same signal for the free ligand. However, the influence of the coordination environment is more marked on the C*H*(CH_3) proton and is characterised by a *ca.* 1.0 ppm shift downfield compared with the same signal for the free ligand. Similar effects have been noted in other systems containing this ligand set.[15] The dimeric or monomeric nature of the complex had no influence on this feature. Complex **2** displayed the largest shift, probably due to the presence of the strong electron withdrawing groups on the alkoxide moiety.

The IR spectra of **1–11** all display a $\nu_{(V\text{–}N)}$ band at around 1160 cm^{-1}, comparable to the IR stretch recorded for $[CpVCl_2\{N\text{-}2,6\text{-}(i\text{-}Pr)_2C_6H_3\}]$ (1157 cm^{-1}) and $[VCl_3\{N\text{-}2,6\text{-}(i\text{-}Pr)_2C_6H_3\}]$ (1143 cm^{-1}).[16] The ^{51}V NMR spectra of complexes bearing an isopropoxide ligand (*i.e.* **4–7**) were consistent with observations made by Moriuchi and Hirao and previously by Maatta.[5,7] When the *para*-arylimido substituent is an electron donating group

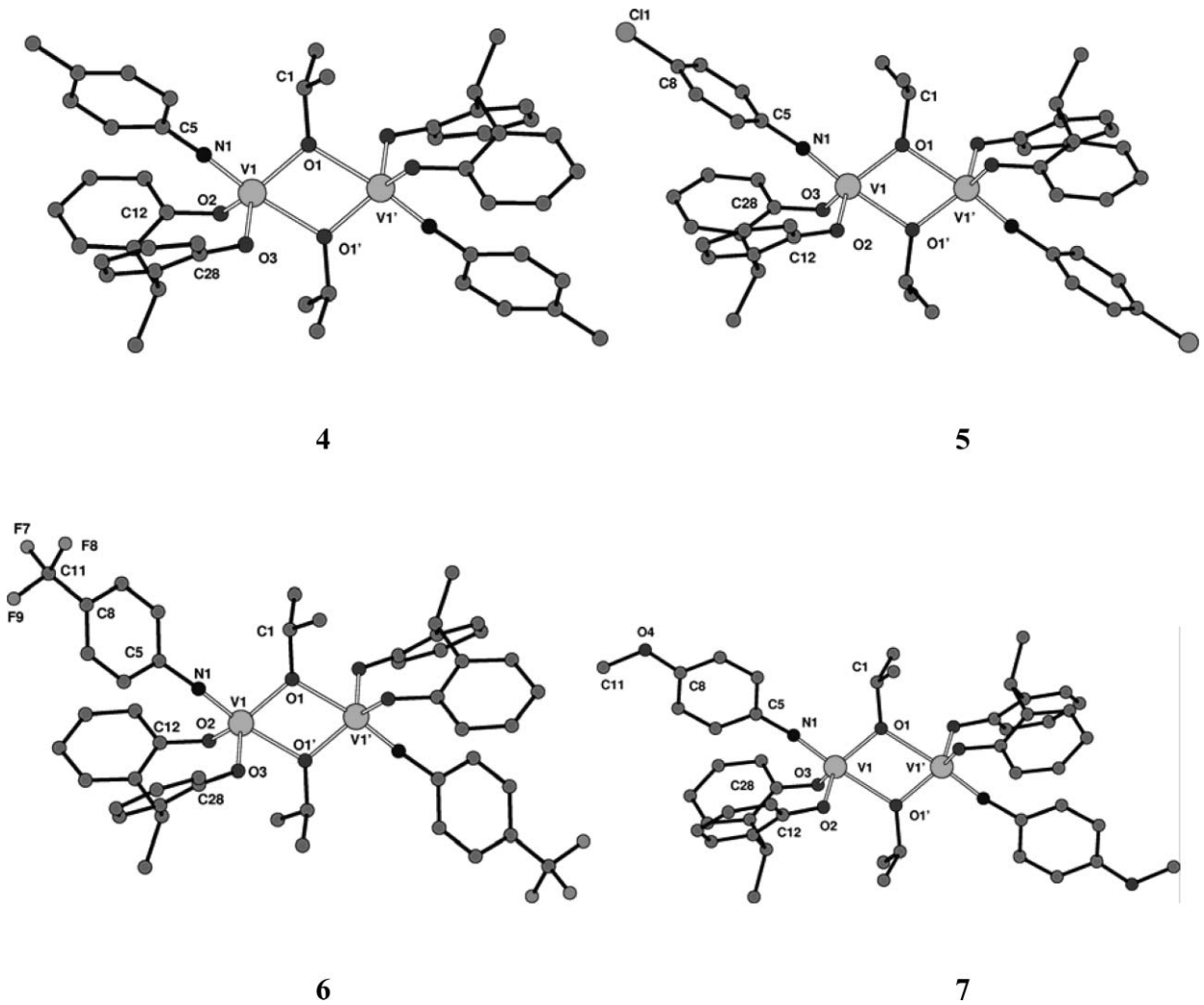

Fig. 4 CAMERON representation of the structures of **8**, **9** and **10** showing spheres of arbitrary size; hydrogen atoms, *t*-Bu groups on the phenolates and solvent molecules of crystallisation have been omitted for clarity.

Table 3 Selected bond lengths and angles for **8–10**

	8	**9**	**10**[a]
Bond lengths/Å			
V(1)–N(1)	1.661(3)	1.677(3)	1.666(3)[b]
V(1)–O(1)	1.885(3)	1.868(2)	1.879(2)[b]
V(1)–O(2)	1.836(2)	1.844(2)	1.829(2)[b]
V(1)–O(3)	1.856(3)	1.824(2)	1.839(2)[b]
V(1)–O(1′)	2.172(2)	2.193(2)	2.181(2)[b]
V(1)···V(1′)	3.281	3.283	3.294
Bond angles/°			
N(1)–V(1)–O(1)	99.34(13)	101.17(11)	100.72(14)[b]
N(1)–V(1)–O(2)	99.11(13)	97.48(12)	98.46(14)[b]
N(1)–V(1)–O(3)	98.05(14)	97.48(12)	98.43(14)[b]
N(1)–V(1)–O(1′)	170.74(13)	173.31(11)	171.97(14)[b]
O(1)–V(1)–O(2)	117.55(11)	124.05(10)	118.29(13)[b]
O(1)–V(1)–O(3)	125.04(11)	117.14(10)	124.34(12)[b]
O(1)–V(1)–O(1′)	72.27(11)	72.37(10)	71.76(11)[b]
O(2)–V(1)–O(3)	110.39(12)	111.19(10)	109.67(13)[b]
V(1)–O(1)–V(1′)	107.73(11)	107.63(10)	108.24(11)[b]
V(1)–N(1)–C(5)	178.4(3)	174.0(2)	175.7(3)[b]

[a] Lacks a crystallographic centre of symmetry. [b] Average of two values in non-symmetrical molecule.

Table 4 Selected spectroscopic data[a]

Compound	CH(CH_3) δ ^{1}H NMR/ ppm	CH(CH_3) δ ^{1}H NMR/ ppm	δ ^{51}V NMR/ ppm ($\omega_{1/2}$/Hz)	IR $\nu_{(V–N)}$/ cm^{-1}
1	1.63	5.51	–544 (120) –538 (360)[b]	1157
2	1.67	5.64	–315 (120) –317 (500)[b]	1157
3	1.61	5.46	–414 (514)	1157
4	1.62	5.46	–384 (466)	1156
5	1.55	5.43	–396 (470)	1157
6	1.59	5.43	–413 (260)	1156
7	1.62	5.46	–361 (365)	1163
8	1.67	5.45	–443 (650)	1157
9	1.67	5.42	–504 (428)	1158
10	1.60	5.47	–503 (80)	1156
11	1.65	5.50	–154 (1800)	1157
LH_2	1.69	4.45	—	—

[a] NMR data collected in $CDCl_3$ at room temperature; IR data collected in nujol on KBr plates. [b] Collected in C_6D_6.

(*i.e.* OCH_3 or CH_3) a marked downfield shift for the ^{51}V NMR signal occurs (*e.g.* –361 ppm (**7**) and –384 ppm (**4**)), compared with the ^{51}V NMR signal recorded with electron withdrawing groups such as Cl or CF_3 (*e.g.* –396 ppm (**5**) and –413 (**6**) ppm). Spectroscopic data relevant to this discussion have been collated in Table 4.

Ethylene polymerisation

Complexes **1–11** have been evaluated as pro-catalysts for the polymerisation of ethylene, employing either MAO (methylaluminoxane), TMA (trimethylaluminium) or DMAC (dimethylaluminium chloride) as co-catalyst, and with or without ETA (ethyltrichloroacetate) present. Polymerisations were carried out in toluene (50 mL) using 10 000–50 000 molar equiv. of co-catalyst over a range of temperatures (0–80 °C) over 30 min unless otherwise stated. Representative results are presented in Tables 5 and 6 (see ESI for complete set of polymerisation runs)† and lifetime studies are presented in Fig. 5.

Table 5 Ethylene polymerisation data for pro-catalysts **1–11**[a]

Run	Pro-catalyst	Polymer yield/g	Activity/g PE mmol^{-1} [V] h^{-1} bar^{-1}	M_n/g mol^{-1}	PDI
1	**1**	0.94	37 600	115 000	2.6
2	**2**	0.40	15 850	58 000	4.0
3	**3**	1.17	46 800	146 000	4.1
4	**4**	0.97	38 800	165 000	2.2
5	**5**	1.27	50 800	196 000	2.4
6	**6**	1.36	54 400	200 000	2.3
7	**7**	1.20	48 000	160 000	2.4
8	**8**	1.88	75 200	162 000	2.6
9	**9**	0.68	27 200	78 300	2.6
10	**10**	0.42	16 800	161 000	2.2
11	**11**	1.52	60 800	137 000	2.4

[a] Conditions: 50 mL toluene, 0.1 mL ETA, co-catalyst DMAC 2 mL (40 000 equivalents), 0.05 μmol pro-catalyst, 45 °C, 30 min.

Table 6 Ethylene polymerisation data for complex **6**[a]

Run	Co-catalyst equivalent	T/°C	Polymer yield/g	Activity/g PE mmol^{-1} [V] h^{-1} bar^{-1}	M_n/g mol^{-1}	PDI
1	40 000	25	0.48	38 400	165 000	4.7
2[b]	40 000	25	0.02	1600	165 000	4.1
3	10 000	25	0.04	3200	234 000	2.7
4	20 000	25	0.13	10 400	202 000	3.2
5	30 000	25	0.26	20 800	411 000	2.5
6	50 000	25	0.21	16 800	358 000	3.0
7	40 000	0	0.005	400	—	—
8	40 000	45	0.52	41 600	216 000	2.2
9	40 000	60	0.61	48 800	124 000	2.4
10	40 000	80	0.67	53 600	37 000	2.6

[a] Conditions: 50 mL toluene, 0.1 mL ETA, co-catalyst DMAC (1 M in hexanes), 0.05 μmol pro-catalyst, 15 min. [b] Without ETA.

For complexes **1–11**, it was found that treatment with DMAC in the presence of ETA afforded highly active ethylene polymerisation systems. Such a combination of reagents has proved to be beneficial for producing highly active vanadium-based systems, as reported by both us[13,17] and others.[18] Treatment of pro-catalyst **6** with either TMA or MAO resulted in little or no polymer formation, even in the presence of the reactivator ETA. The dramatic effect of ETA on the polymerisation is illustrated by run 1 (Table 6), whereas in the absence of ETA, the activity of pro-catalyst **6** is only approximately 4% of that obtained when ETA is present in the system (Table 6, run 2).

A comparative study was conducted under the same conditions for complexes **1** and **2** in order to assess their respective polymerisation behaviour due to their differing alkoxides, independent of variation of other parameters. The results are collated in Table 7, and reveal that whilst the initial activity is higher for the hexafluoro-*tert*-butoxide pro-catalyst **2**, the system utilising the *tert*-butoxide **1** has a significantly enhanced performance over time. Data from Table 5 also suggest that use of a *p*-CH_3 substituent on the arylimido group is beneficial for enhanced activity (Table 5, entries 8–11).

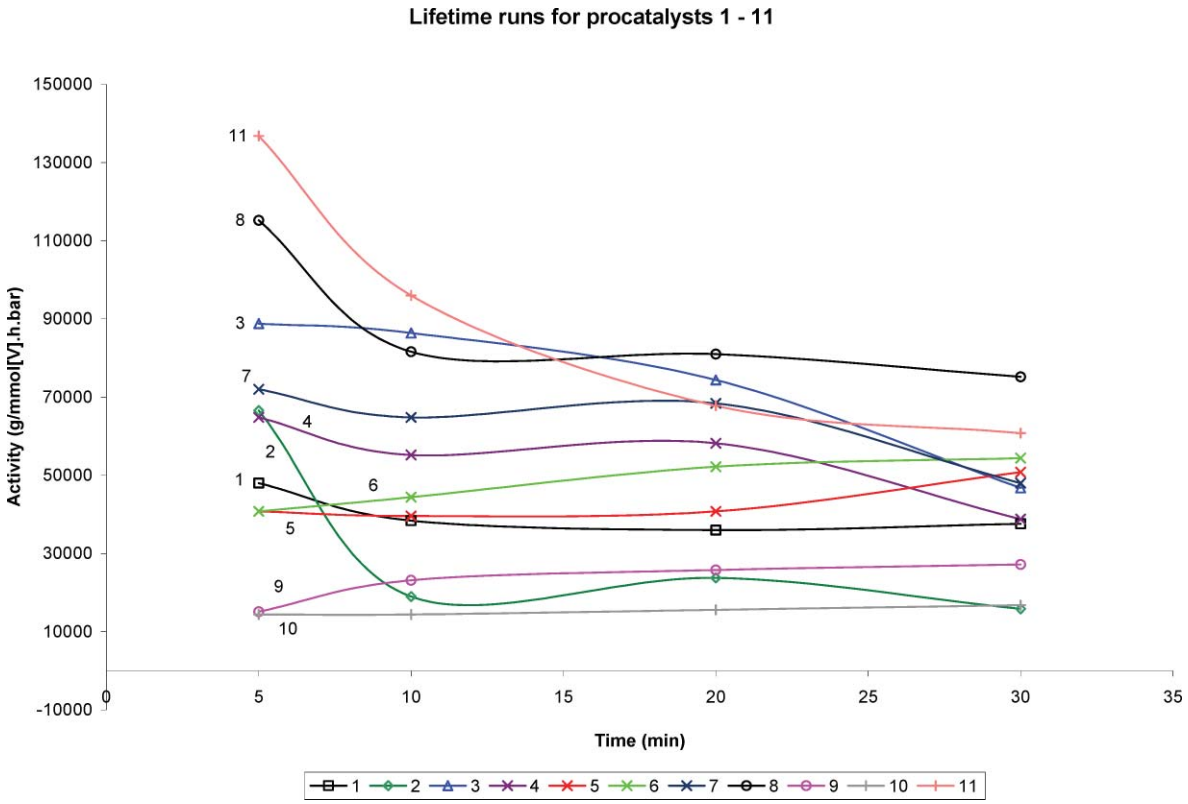

Fig. 5 Lifetime studies for pro-catalysts **1**–**11**. Conditions: 50 mL toluene, 0.1 mL ETA, co-catalyst DMAC 2 mL (40 000 equivalents), 0.05 μmol pro-catalyst, 45 °C.

Table 7 Comparative runs for pro-catalysts **1** and **2**[a]

Run	Pro-catalyst	Polymer yield/g	Activity/g PE mmol^{-1}[V] h^{-1} bar^{-1}	M_n/g mol^{-1}	PDI
1[b]	**1**	0.20	48 000	—	—
2[c]	**1**	0.94	37 600	115 000	2.6
3[b]	**2**	0.28	66 560	—	—
4[c]	**2**	0.40	15 850	58 000	4.0

[a] Conditions: 50 mL toluene, 0.1 mL ETA, cocatalyst DMAC 2 mL (40 000 equivalents), 0.05 μmol procatalyst, 45 °C. [b] 5 min; [c] 30 min.

ε-Caprolactone polymerisation

Complexes **1–11** were also screened for their ability to polymerise ε-caprolactone. Complex **7** was subjected to temperature and co-initiator concentration studies. The polymerisation data are presented in Table 8.

Complex **7** was active for the ring opening polymerisation of ε-caprolactone. However, it was only moderately active at room temperature, leading to low conversions after 24 h (Table 8, entry 1). The conversion increased dramatically with temperature, without noticeable increase of polydispersity index. (Table 8, entries 2 and 3). Complex **7** was also active at low catalyst loading leading to 29% conversion after 24 h for 900 equivalents of monomer.

All polymers obtained were of low polydispersity (IP $\leq$ 1.3), which suggested that these polymerisations occurred without side reactions. Interestingly, only low molecular weight polymers were obtained using this alkoxy vanadium/benzyl alcohol system.

In order to investigate the influence of the co-initiator on the catalyst performance, the polymerisation was run both in the absence of benzyl alcohol (Table 8, entry 7) and with an excess of benzyl alcohol present (Table 8, entry 8). Results revealed that the concentration of benzyl alcohol had little effect on the catalytic activity: after 24 h at 40 °C, the conversions obtained ranged from 41 to 50% (Table 8, entries 7, 2 and 8 for 0, 1 and 2 equivalents of co-initiator, respectively). In the absence of benzyl alcohol, a three-fold increase of the molecular weight was noted without the increase in polydispersity index described with other metals operating under such conditions.[19]

The screening of complexes **1–11** (Table 9) revealed that the monomeric complexes (*i.e.* **1–3**) showed lower activities than their dimeric analogues (*i.e.* **4–11**). After 24 h, complexes **1–3** afforded only low conversions ($\leq$25%), whereas higher conversions (41–78%) were reached using complexes **4–11** under similar conditions.

Given that the propagating species is likely to be monomeric (the growing polymeric chain is bulkier than a *tert*-butyl group), we propose that the beneficial effect evidenced here involves the initiation step of the polymerisation, when the first monomer is coordinated to the metal and inserted into the V–OR bond. For complexes bearing the same alkoxide ligand, the *para*-arylimido substituent has little effect on the polymerisation activity; however, some activity trends can be drawn here. For instance, when the alkoxy group is an isopropoxide, the catalytic activity followed the order: $CH_3 \approx CF_3 > Cl > OCH_3$. For dimeric complexes (*i.e.*

Table 8 ε-Caprolactone polymerisation data for complex **7**[a]

Run	Monomer/metal	T/°C	Conversion[b](%)	M_n calculated/g mol^{-1}	M_n measured[c]/g mol^{-1}	PDI
1	500	25	7	4000	—	—
2	500	40	41	23 450	5510	1.1
3	500	60	82	46 900	9420	1.2
4	300	40	77	26 430	7410	1.1
5	700	40	42	33 640	8690	1.1
6	900	40	29	29 860	5760	1.3
7[d]	500	40	50	28 600	16 900	1.1
8[e]	500	40	47	13 440	5760	1.1

[a] Conditions: 40 mL of toluene; 5 mL of ε-caprolactone; 1 equivalent of benzyl alcohol (from a 0.97 M solution in toluene). [b] Calculated by ^{1}H NMR. [c] M_n measured = 0.45 × M_n GPC. [d] No benzyl alcohol. [e] 2 equivalents of benzyl alcohol.

Table 9 ε-Caprolactone polymerisation data for complexes **1–11**[a]

Run	Pro-catalyst	Conversion[b] (%)	M_n calculated/ g mol^{-1}	M_n measured[c]/ g mol^{-1}	PDI
1	**1**	13	7440	4390	1.1
2	**2**	0	—	—	—
3	**3**	25	14 300	8460	1.1
4	**4**	64	36 610	7830	1.1
5	**5**	53	30 320	8110	1.3
6	**6**	60	34 320	8050	1.1
7	**7**	41	23 450	5510	1.1
8	**8**	65	37 180	10 940	1.1
9	**9**	78	44 620	7920	1.2
10	**10**	74	42 330	15 040	1.3
11	**11**	73	41 760	11 860	1.1

[a] Conditions: monomer/metal = 500; 40 mL of toluene; 5 mL of ε-caprolactone; 1 equivalent of benzyl alcohol (from a 0.97 M solution in toluene); 40 °C. [b] Calculated by ^{1}H NMR. [c] M_n measured = 0.45 × M_n GPC.

4–10), the observed catalytic activity increased with the upfield shift of the ^{51}V NMR signal (Fig. 6). Complex **11** was excluded from this correlation because of the atypical wide broadening of the ^{51}V NMR signal ($\omega_{1/2}$ = 1800 Hz).

However, the electronic effect alone is not sufficient to explain the variations in activity. Other factors, relating to the nature of the alkoxide ligand have an influence on the polymerisation process. For example, we noted that complexes with an ethoxide ligand displayed better activities (in terms of conversion) than complexes with the longer alkoxy group *n*-propoxide (Table 9, entries 8 and 11). Furthermore, the position of the electron withdrawing groups on the ligand framework is of key importance. Most notably, the use of the fluorinated alkoxide $OC(CH_3)(CF_3)_2$ led to complete de-activation of the complex for ε-caprolactone polymerisation (Table 9, entry 2 *vs.* entry 1). In this particular case, the enhanced Lewis acidity of the metal centre is counter-balanced by the reduced nucleophilicity of the alkoxide group.

In conclusion, crystal structure determinations for complexes of the form $[V(NAr)L(OR)]_n$ have shown that when the alkoxide is *tert*-butoxide (or the fluorinated derivative thereof), a monomeric (n = 1) structure results, whereas for less bulky alkoxides, such as ethoxy or propoxy groups, a dimeric structure (n = 2) is formed. In combination with DMAC and ETA, such arylimido vanadium complexes afford highly active (up to 75 000 g mmol^{-1} h^{-1} bar^{-1}) systems for polyethylene production. The use of fluorinated *tert*-butoxides leads to improved initial activity, whilst the variation

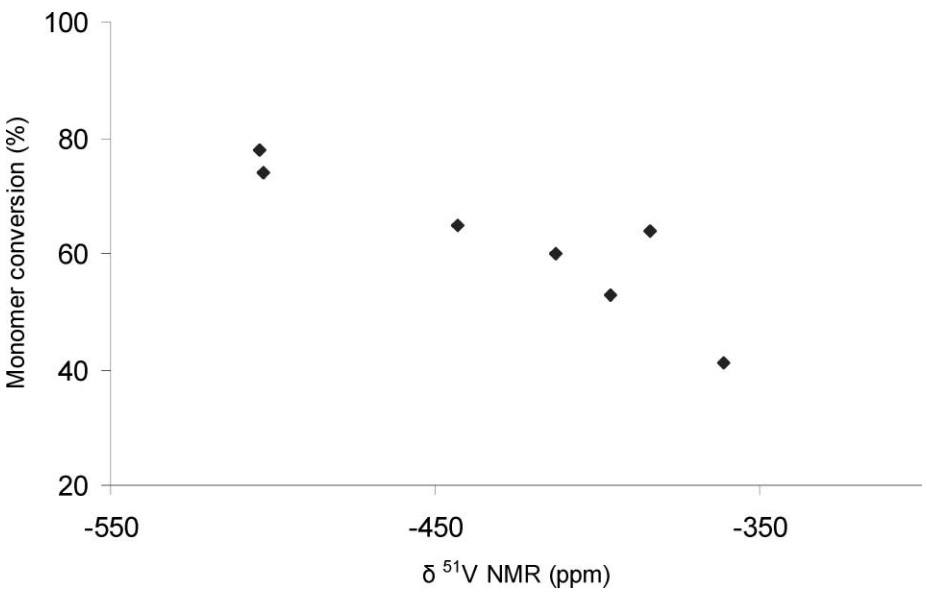

Fig. 6 Monomer conversion (%) with the ^{51}V NMR chemical shift (ppm) for complexes **4–10**.

Compound	**1**	**2**	**3**	**4**	**5**	**6**	**7**	**8**·2(CH_2Cl_2)	**9**·CH_3CN	**10**·CH_2Cl_2
Formula	$C_{41}H_{60}NO_3V$	$C_{41}H_{54}F_6NO_3V$	$C_{40}H_{57}ClNO_3V$	$C_{80}H_{116}N_2O_6V_2$	$C_{78}H_{110}Cl_2N_2O_6V_2$	$C_{80}H_{110}F_6N_2O_6V_2$	$C_{80}H_{116}N_2O_8V_2$	$C_{80}H_{116}N_2O_6V_2$, 2(CH_2Cl_2)	$C_{80}H_{110}F_6N_2O_6V_2$, C_2H_3N	$C_{76}H_{106}Cl_2N_2O_6V_2$, CH_2Cl_2
M_r	665.84	773.79	686.26	1303.63	1344.46	1411.58	1335.63	1473.48	1452.63	1401.33
Crystal system	Monoclinic	Monoclinic	Monoclinic	Monoclinic	Monoclinic	Monoclinic	Triclinic	Orthorhombic	Triclinic	Monoclinic
Space group	$C2/m$	$P2_1$	$C2/c$	$P2_1/c$	$P2_1/c$	$C2/c$	$P\bar{1}$	$Pbca$	$P\bar{1}$	$P2_1/n$
a/Å	10.9243(7)	10.2039(6)	18.2831(8)	9.6738(7)	9.8290(5)	10.7533(8)	10.6184(3)	19.206(2)	10.5771(10)	19.0504(18)
b/Å	18.3726(11)	19.5337(11)	11.0322(4)	17.4718(12)	17.5429(9)	18.7325(14)	10.6968(4)	19.9382(17)	10.9292(16)	19.7366(19)
c/Å	20.1620(12)	10.3267(6)	41.0433(19)	22.3216(17)	21.4878(12)	38.124(2)	16.6833(7)	21.798(2)	17.8899(15)	20.978(2)
α/°	90	90	90	90	90	90	91.325(3)	90	100.193(10)	90
β/°	90.7902(11)	91.0073(9)	98.0783(12)	96.642(7)	94.687(5)	91.883(6)	95.727(3)	90	94.794(7)	99.969(8)
γ/°	90	90	90	90	90	90	91.217(3)	90	96.548(10)	90
V/Å^3	4046.3(4)	2058.0(2)	8196.4(6)	3747.4(5)	3692.7(3)	7675.4(9)	1884.45(12)	8347.2(14)	2010.7(4)	7768.4(13)
Z	4	2	8	2	2	4	1	4	1	4
T/K	150(2)	150(2)	120(2)	140(2)	140(2)	140(2)	140(2)	140(2)	140(2)	140(2)
No. data collected	18044	24199	28806	41164	42947	42244	25919	70865	26731	83922
No. unique data	5043	12114	6959	6590	8590	6733	8611	7425	9182	13785
R_{int}	0.0252	0.0219	0.0474	0.1726	0.0925	0.1339	0.0637	0.2251	0.0650	0.1336
R_1 [$F^2 > 2\sigma(F^2)$]	0.0428	0.0411	0.0639	0.0535	0.0452	0.0540	0.0421	0.0739	0.0671	0.0495
wR_2 (all data)	0.1175	0.1109	0.1364	0.1208	0.0811	0.1161	0.0851	0.1162	0.1970	0.0792

of the *para* substituent on the arylimido group revealed higher activities for *p*-CF_3 and *p*-Cl. In the case of ε-caprolactone polymerisation, better conversions (≥ 60%) were achieved using dimeric pro-catalysts possessing propoxide bridges (complexes **4**–**8**), whereas far poorer conversions (≤ 25%) were observed when using monomeric pro-catalysts (complex **2** was inactive).

Experimental

General

All manipulations were carried out under an atmosphere of dinitrogen using standard Schlenk and cannula techniques or in a conventional nitrogen-filled glove-box. Solvents were refluxed over an appropriate drying agent and distilled and degassed prior to use. Elemental analyses were performed by the microanalytical services at London Metropolitan University. NMR spectra were recorded on a Varian VXR 400 S spectrometer at 400 MHz (^{1}H) and 105.1 MHz (^{51}V) or a Gemini 300 NMR spectrometer at 300 MHz (^{1}H) and 282.4 MHz (^{19}F) at 298 K; chemical shifts are referenced to the residual protio impurity of the deuterated solvent (^{1}H NMR) or to an external $VOCl_3$/$CDCl_3$ reference (^{51}V NMR). IR spectra (Nujol mulls, KBr windows) were recorded on Perkin-Elmer 577 and 457 grating spectrophotometers. Number and weight average molecular weights (M_n and M_w) for all poly(ε-caprolactone) samples were measured by gel permeation chromatography (GPC) on a Polymer Laboratories PL GPC 220 instrument equipped with PL gel 5 Å mixed C column eluted in tetrahydrofuran at 1.0 mL min^{-1} at 40 °C and calibrated using nine monodisperse polystyrene standards in the range 580–1 233 000 Da. The complexes [V(NAr)(O*t*-Bu)$_3$], [V(NAr)(OC(CH$_3$)(CF$_3$)$_2$)$_3$] and [V(NAr)(OR)$_3$] (R = Et, *n*-Pr, *i*-Pr) were prepared as described in the literature.[7] All other chemicals were obtained commercially and used as received unless stated otherwise.

Synthesis of [V(N*p*-tolyl)(L)(O*t*-Bu)] (1). [V(N*p*-tolyl)(O*t*-Bu)$_3$] (0.94 g, 2.51 mmol) and LH_2 (1.00 g, 2.28 mmol) were refluxed in toluene (40 mL) for 12 h. Upon cooling the solution, the volatiles were removed *in vacuo* and the residue was washed with cold acetonitrile (40 mL). Recrystallisation from a saturated acetonitrile solution, after standing at ambient temperature for 1–2 d afforded **1** as orange prisms. Yield: 0.68 g, 45%; mp. 186 °C (decomposition). Elemental analysis calculated for $C_{41}H_{60}NO_3V$: C 73.96, H 9.08, N 2.10; found: C 73.91, H 8.93, N 2.05%. ^{1}H NMR ($CDCl_3$, 400 MHz) δ: 7.57 (s, 2 H, C_6H_2), 7.02 (s, 2 H, C_6H_2), 6.45 (d, 2 H, J = 8.1 Hz, NC_6H_4), 5.67 (d, 2 H, J = 8.1 Hz, NC_6H_4), 5.51 (q, 1 H, J = 7.3 Hz, $CHCH_3$), 2.12 (s, 3 H, $CH_3C_6H_4N$), 1.63 (m, 12 H, $OC(CH_3)_3$ and $CHCH_3$), 1.30 (s, 36 H, $C(CH_3)_3$) ppm. ^{51}V NMR (C_6D_6, 105.1 MHz) δ: −538.10 ppm ($\omega_{1/2}$ 360 Hz). ^{51}V NMR ($CDCl_3$, 105.1 MHz) δ: −543.73 ppm ($\omega_{1/2}$ 120 Hz). MS (MALDI): m/z 665 [M$^+$], 591 [M$^+$ − O*t*-Bu]. IR (KBr, Nujol mull): 1596 (w), 1359 (s), 1258 (s), 1227 (m), 1157 (s), 1106 (m), 1005 (s), 887 (m), 846 (m), 800 (s), 772 (m), 753 (m), 687 (m), 664 (m), 652 (m), 629 (m), 617 (m), 590 (m) cm^{-1}.

Synthesis of [V(N*p*-tolyl)(L)(OC(CF$_3$)$_2$Me)] (2). As for **1**, but using [V(N*p*-tolyl)(OC(CF$_3$)$_2$Me)$_3$] (1.49 g, 2.1 mmol) and LH_2 (0.85 g, 1.9 mmol) affording **2** as orange/red prisms. Yield: 0.60 g, 40%; mp. 128 °C. Elemental analysis calculated for

$C_{41}H_{54}F_6NO_3V$: C 63.64, H 7.03, N 1.81; found: C 63.77, H 6.97, N 1.90%. ^{1}H NMR ($CDCl_3$, 400 MHz) δ: 7.62 (s, 2 H, C_6H_2), 6.90 (s, 2 H, C_6H_2), 6.11 (d, 2 H, J = 8.2 Hz, NC_6H_4), 5.64 (q, 1 H, J = 7.2 Hz, $CH(CH_3)$), 4.66 (d, 2 H, J = 8.2 Hz, NC_6H_4), 2.00 (s, 3 H, $CH_3C_6H_4N$), 1.96 (s, 3 H, $C(CH_3)(CF_3)_2$), 1.67 (d, 3 H, J = 7.2 Hz, $CH(CH_3)$), 1.36 (s, 18 H, $C(CH_3)_3$), 1.29 (s, 18 H, $C(CH_3)_3$) ppm. ^{51}V NMR ($CDCl_3$, 105.1 MHz) δ: –315.40 ppm ($\omega_{1/2}$ 120 Hz). ^{51}V NMR (C_6D_6, 105.1 MHz) δ: –316.53 ppm ($\omega_{1/2}$ 500 Hz).^{19}F NMR ($CDCl_3$, 282.4 MHz) δ: –77.81 ppm. MS (EI): m/z 773.2 [M$^+$]. IR (Nujol mull, KBr): 1599 (w), 1514 (m), 1309 (m), 1293 (m), 1262 (s), 1214 (w), 1192 (w), 1157 (m), 1094 (s), 1021 (s), 975 (m), 934 (w), 879 (w), 800 (s), 735 (w), 722 (m) cm^{-1}.

Synthesis of [V(N*p*-(Cl)C_6H_4)(L)(O*t*-Bu)] (3). As for **1**, but using [V(N*p*-(Cl)C_6H_4)(O*t*-Bu)$_3$] (1.27 g, 3.2 mmol) and LH_2 (1.27 g, 2.9 mmol) affording **3** as orange/red prisms. Yield: 1.17 g, 59%; mp. 122 °C. Elemental analysis calculated for $C_{40}H_{57}ClNO_3V$: C 70.01, H 8.37, N 2.04; found: C 69.86, H 8.38, N 1.90%. ^{1}H NMR ($CDCl_3$, 400 MHz) δ: 7.56 (s, 2 H, C_6H_2), 7.03 (s, 2 H, C_6H_2), 6.62 (d, 2 H, J = 8.6 Hz, NC_6H_4), 5.66 (d, 2 H, J = 8.6 Hz, NC_6H_4), 5.46 (q, 1 H, J = 7.2 Hz, $CHCH_3$), 1.61 (m, 12 H, $OC(CH_3)_3$ and $CHCH_3$), 1.29 (s, 36 H, $C(CH_3)_3$) ppm. ^{51}V NMR (105.1 MHz, $CDCl_3$) δ: –414.2 ppm ($\omega_{1/2}$ 514 Hz). MS (EI): m/z 686.3 [M]$^+$. IR (Nujol mull, KBr): 1260 (s), 1228 (w), 1200 (w), 1157 (m), 907 (m), 878 (w), 869 (w), 849 (m), 770 (w), 757 (w), 737 (w), 689 (w), 654 (w), 636 (m), 6199 (w), 594 (m) cm^{-1}.

Synthesis of [V(N*p*-tolyl)(L)(O*i*-Pr)]$_2$ (4). As for **1**, but using [V(N*p*-tolyl)(O*i*-Pr)$_3$] (0.70 g, 2.1 mmol) and LH_2 (0.85 g, 1.9 mmol) affording **4** as orange/red prisms. Yield: 0.86 g, 68%; mp. 98 °C. Elemental analysis calculated for $C_{40}H_{58}NO_3V$: C 73.70, H 8.97, N 2.15; found: C 73.62, H 8.43, N 2.15%. ^{1}H NMR ($CDCl_3$, 400 MHz) δ: 7.57 (s, 2 H, C_6H_2), 7.02 (s, 2 H, C_6H_2), 6.46 (d, 2 H, J = 8.2 Hz, NC_6H_4), 5.65 (d, 2 H, J = 8.2 Hz, NC_6H_4), 5.46 (m, 2 H, $CHCH_3$ and $CH(CH_3)_2$), 2.12 (s, 3 H, $CH_3C_6H_4$), 1.62 (d, 3 H, J = 7.3 Hz, $CHCH_3$), 1.55 (d, 6 H, J = 6.1 Hz, $CH(CH_3)_2$), 1.30 (s, 36 H, $C(CH_3)_3$) ppm. ^{51}V NMR (105.1 MHz, $CDCl_3$) δ: –383.5 ppm ($\omega_{1/2}$ 466 Hz). MS (EI): m/z 651.3 [M]$^+$. IR (Nujol mull, KBr): 1260 (s), 1227 (m), 1201 (w), 1156 (w), 910 (m), 867 (m), 752 (w), 638 (m), 614 (w), 580 (w) cm^{-1}.

Synthesis of [V(N*p*-ClC$_6H_4$)(L)(O*i*-Pr)]$_2$ (5). As for **1**, but using [V(N*p*-(Cl)C_6H_4)(O*i*-Pr)$_3$] (0.74 g, 2.1 mmol) and LH_2 (0.84 g, 1.9 mmol) affording **5** as orange/red prisms. Yield: 0.98 g, 76%; mp. 96 °C. Elemental analysis calculated for $C_{39}H_{55}ClNO_3V$: C 69.68, H 8.25, N 2.08; found: C 69.82, H 8.36, N 2.02%. ^{1}H NMR ($CDCl_3$, 400 MHz) δ: 7.57 (s, 2 H, C_6H_2), 7.04 (s, 2 H, C_6H_2), 6.63 (d, 2 H, J = 8.6 Hz, NC_6H_4), 5.65 (d, 2 H, J = 8.6 Hz, NC_6H_4), 5.43 (m, 2 H, $CHCH_3$) and $CH(CH_3)_2$), 1.62 (d, 3 H, J = 7.3 Hz, $CHCH_3$), 1.55 (d, 6 H, J = 6.1 Hz, $CH(CH_3)_2$), 1.30 (s, 36 H, $C(CH_3)_3$) ppm. ^{51}V NMR (105.1 MHz, $CDCl_3$) δ: –395.9 ppm ($\omega_{1/2}$ 470 Hz). MS (EI): m/z 672.3 [M]$^+$. IR (Nujol mull, KBr): 1568 (w), 1261 (m), 1224 (w), 1157 (w), 1109 (m), 1090 (m), 1014 (m), 932 (w), 881 (w), 866 (w), 824 (m), 802 (s), 773 (w), 752 (w), 731 (m), 689 (w), 637 (m), 596 (w), 580 (m), 570 (m) cm^{-1}.

Synthesis of [V(N*p*-(CF$_3$)C_6H_4)(L)(O*i*-Pr)]$_2$ (6). As for **1**, but using [V(N*p*-(CF$_3$)C_6H_4)(O*i*-Pr)$_3$] (0.81 g, 2.1 mmol) and LH_2 (0.85 g, 1.9 mmol) affording **6** as orange/red prisms. Yield: 0.62 g, 45%; mp. 100 °C. Elemental analysis calculated for $C_{40}H_{55}F_3NO_3V$: C 68.07, H 7.85, N 1.98; found: C 68.12, H 7.75, N 1.94%. ^{1}H NMR ($CDCl_3$, 400 MHz) δ: 7.57 (s, 2 H, C_6H_2), 7.04 (s, 2 H, C_6H_2), 6.93 (d, 2 H, J = 8.3 Hz, NC_6H_4), 5.79 (d, 2 H, J = 8.3 Hz, NC_6H_4), 5.43 (m, 2 H, $CHCH_3$ and $CH(CH_3)_2$), 1.59 (d, 3 H, J = 7.2 Hz, $CHCH_3$), 1.55 (d, 6 H, J = 6.1 Hz, $CH(CH_3)_2$), 1.31 (s, 18 H, $C(CH_3)_3$), 1.29 (s, 18 H, $C(CH_3)_3$) ppm. ^{51}V NMR (105.1 MHz, $CDCl_3$) δ: –413.17 ppm ($\omega_{1/2}$ 260 Hz). MS (EI): m/z 705.3 [M]$^+$. IR (Nujol mull, KBr): 1238 (m), 1294 (m), 1261 (s), 1245 (w), 1226 (m), 1212 (w), 1156 (m), 992 (m), 922 (w), 907 (m), 877 (w), 864 (w), 851 (m), 769 (w), 689 (w), 661 (m), 638 (w), 595 (w) cm^{-1}.

Synthesis of [V(N*p*-(OMe)C_6H_4)(L)(O*i*-Pr)]$_2$ (7). As for **1**, but using [V(N*p*-(OMe)C_6H_4)(O*i*-Pr)$_3$] (1.05 g, 3.0 mmol) and LH_2 (1.18 g, 2.7 mmol) affording **7** as orange/red prisms. Yield: 1.38 g, 77%; mp. 92 °C. Elemental analysis calculated for $C_{40}H_{58}NO_4V$: C 71.94, H 8.75, N 2.10; found: C 71.84, H 8.83, N 1.90%. ^{1}H NMR (300 MHz, $CDCl_3$) δ: 7.59 (s, 2 H, C_6H_2), 7.02 (s, 2 H, C_6H_2), 6.15 (d, 2 H, J = 8.9 Hz, NC_6H_4), 5.72 (d, 2 H, J = 8.9 Hz, NC_6H_4), 5.46 (m, 2 H, $CH(CH_3)$ and $CH(CH_3)_2$), 3.60 (s, 3 H, $CH_3OC_6H_4$), 1.62 (d, 3 H, J = 7.3 Hz, $CH(CH_3)$), 1.55 (d, 6 H, J = 6.2 Hz, $CH(CH_3)_2$), 1.30 (s, 36 H, $C(CH_3)_3$) ppm. ^{51}V NMR (105.1 MHz, $CDCl_3$) δ: –360.5 ppm ($\omega_{1/2}$ 365 Hz). MS (EI): m/z 667.3 [M]$^+$.IR (Nujol mull, KBr): 1587 (m), 1512 (w), 1299 (w), 1261 (m), 1228 (w), 1163 (m), 1105 (s), 1035 (s), 914 (w), 802 (s), 722 (w), 635 (w) cm^{-1}.

Synthesis of [V(N*p*-tolyl)(L)(O*n*-Pr)]$_2$ (8). As for **1**, but using [V(N*p*-tolyl)(O*n*-Pr)$_3$] (0.70 g, 2.1 mmol) and LH_2 (0.84 g, 1.9 mmol) affording **8**·2(CH_2Cl_2) as orange/red prisms after recrystallisation from CH_2Cl_2. Yield: 0.98 g, 79%; mp. 118 °C. Elemental analysis calculated for $C_{40}H_{58}NO_3V$ (sample dried *in-vacuo* for 12 h, –2 CH_2Cl_2): C 73.70, H 8.97, N 2.15; found: C 73.82, H 8.88, N 2.23%. ^{1}H NMR (400 MHz, $CDCl_3$) δ: 7.61 (s, 2H, C_6H_2), 6.99 (s, 2H, C_6H_2), 6.42 (d, 2 H, J = 8.2 Hz, NC_6H_4), 5.62 (d, 2 H, J = 8.2 Hz, NC_6H_4), 5.45 (q, 1 H, J = 7.1 Hz, $CH(CH_3)$), 5.34 (m, 2 H, $OCH_2CH_2CH_3$), 2.34 (m, 2 H, $OCH_2CH_2CH_3$), 2.13 (s, 3 H, $CH_3C_6H_4N$), 1.67 (d, 3 H, J = 7.1 Hz, $CH(CH_3)$), 1.41 (s, 18 H, $C(CH_3)_3$), 1.30 (s, 18 H, $C(CH_3)_3$), 0.85 (t, 3 H, $OCH_2CH_2CH_3$) ppm. ^{51}V NMR (105.1 MHz, $CDCl_3$) δ: –442.93 ($\omega_{1/2}$ 650 Hz). MS (EI): m/z 651.3 [M]$^+$. IR (Nujol mull, KBr): 1295 (m), 1261 (w), 1245 (w), 1227 (m), 1202 (w), 1157 (m), 1112 (m), 1038 (m), 1009 (m), 976 (m), 909 (w), 889 (w), 880 (w), 867 (w), 834 (s), 816 (m), 803 (m), 783 (w), 774 (m), 753 (m), 650 (w), 624 (w), 613 (m), 583 (m) cm^{-1}.

Synthesis of [V(N*p*-(CF$_3$)C_6H_4)(L)(O*n*-Pr)]$_2$ (9). As for **1**, but using [V(N*p*-(CF$_3$)C_6H_4)(O*n*-Pr)$_3$] (0.46 g, 1.2 mmol) and LH_2 (0.48 g, 1.1 mmol) affording **9**·CH_3CN as orange/red prisms. Yield: 0.40 g, 52%; mp. 100 °C. Elemental analysis calculated for $C_{40}H_{55}F_3NO_3V$ (sample dried *in-vacuo* for 12 h, –CH_3CN): C 68.07, H 7.85, N 1.98; found: C 68.16, H 7.76, N 1.91%. ^{1}H NMR ($CDCl_3$, 400 MHz) δ: 7.61 (s, C_6H_2), 7.00 (s, 2 H, C_6H_2), 6.91 (d, 2 H, J = 8.3 Hz, NC_6H_4), 5.76 (d, 2 H, J = 8.3 Hz, NC_6H_4), 5.42 (q, 1 H, J = 7.3 Hz, $CHCH_3$), 5.35 (m, 2 H, $OCH_2CH_2CH_3$), 2.33 (m, 2 H, $OCH_2CH_2CH_3$), 1.67 (d, 3 H, J = 7.3 Hz, $CHCH_3$), 1.42 (s, 18 H, $C(CH_3)_3$), 1.29 (s, 18 H, $C(CH_3)_3$), 0.88 (t, 3 H, J = 7.3 Hz, $OCH_2CH_2CH_3$) ppm. ^{51}V NMR (105.1 MHz, $CDCl_3$) δ: –503.5 ppm ($\omega_{1/2}$ 428 Hz). MS (EI): m/z 705.3 [M]$^+$. IR (Nujol mull, KBr): 1324 (m), 1261 (m), 1227 (w), 1158 (m), 1129 (m), 1105 (m), 1069 (w), 1036 (w), 1007 (m), 977 (w), 907 (w), 881 (w),

868 (w), 840 (m), 802 (m), 772 (w), 722 (w), 694 (w), 646 (w), 635 (m), 585 (m) cm^{-1}.

Synthesis of [V(N*p*-ClC$_6$H$_4$)(L)(μ-OEt)]$_2$ (10). As for **1**, but using [V(N*p*-(Cl)C$_6$H$_4$)(OEt)$_3$] (0.53 g, 1.7 mmol) and LH_2 (0.68 g, 1.5 mmol) affording **10**·CH_2Cl_2 as orange/red prisms after recrystallisation from CH_2Cl_2. Yield: 0.52 g, 51%; mp. 97 °C. Elemental analysis calculated for $C_{38}H_{53}ClNO_3V$ (sample dried *in-vacuo* for 12 h, $-CH_2Cl_2$): C 69.34, H 8.12, N 2.13; found: C 69.15, H 7.98, N 2.12%. ^{1}H NMR ($CDCl_3$, 400 MHz) δ: 7.59 (s, 2 H, C$_6H_2$), 7.00 (s, 2 H, C$_6H_2$), 6.61 (d, 2 H, $J = 8.6$ Hz, NC$_6H_4$), 5.67 (d, 2 H, $J =$ 8.6 Hz, NC$_6H_4$), 5.47 (m, 3 H, CH(CH$_3$) and CH_2CH$_3$), 1.74 (t, 3 H, $J = 6.3$ Hz, CH$_2$CH_3), 1.60 (d, 3 H, $J = 7.4$ Hz, CH(CH_3)), 1.42 (s, 18 H, C(CH_3)$_3$), 1.30 (s, 18 H, C(CH_3)$_3$) ppm. ^{51}V NMR (105.1 MHz, $CDCl_3$) δ: −503 ppm ($\omega_{1/2}$ 80 Hz). MS (EI): m/z 658.3 [M]$^+$. IR (Nujol mull, KBr): 1593 (m), 1567 (w), 1293 (m), 1261 (m), 1231 (m), 1201 (w), 1156 (m), 1112 (w), 1087 (m), 1027 (s), 1004 (m), 999 (m), 974 (w), 881 (m), 856 (w), 841 (w), 831 (w), 824 (w), 803 (m), 780 (w), 773 (w), 758 (w), 731 (m), 665 (w), 636 (w) cm^{-1}.

Synthesis of [V(N*p*-tolyl)(L)(μ-OEt)]$_2$ (11). As for **1**, but using [V(N*p*-tolyl)(OEt)$_3$] (0.61 g, 2.1 mmol) and LH_2 (0.84 g, 1.9 mmol) affording **11** as orange/red prisms. Yield: 0.96 g, 79%; mp. 128 °C. Elemental analysis calculated for $C_{39}H_{56}NO_3V$: C 73.44, H 8.85, N 2.20; found: C 73.36, H 8.80, N 2.14%. ^{1}H NMR ($CDCl_3$, 400 MHz) δ: 7.60 (s, 2 H, C$_6H_2$), 6.98 (s, 2 H, C$_6H_2$), 6.42 (d, 2 H, $J = 7.6$ Hz, NC$_6H_4$), 5.66 (d, 2 H, $J = 7.6$ Hz, NC$_6H_4$), 5.50 (m, 3 H, CH(CH$_3$) and CH_2CH$_3$), 2.13 (s, 3 H, CH_3C$_6$H$_4$N), 1.74 (t, 3 H, $J = 6.7$ Hz, CH$_2$CH_3), 1.65 (d, 3 H, $J = 7.0$ Hz, CH(CH_3)), 1.42 (s, 18 H, C(CH_3)$_3$), 1.29 (s, 18 H, C(CH_3)$_3$) ppm. ^{51}V NMR (105.1 MHz, $CDCl_3$) δ: −154.2 ppm ($\omega_{1/2}$ 1800 Hz). MS (EI): m/z 637.3 [M]$^+$. IR (Nujol mull, KBr): 1292 (w), 1261 (w), 1244 (w), 1230 (m), 1201 (m), 1157 (m), 1134 (m), 1112 (m), 1088 (m), 977 (m), 932 (w), 919 (w), 907 (m), 890 (m), 882 (w), 868 (w), 834 (s), 816 (w), 783 (w), 774 (w), 753 (m), 687 (w), 668 (w), 649 (w), 636 (m), 617 (w), 605 (s), 585 (m) cm^{-1}.

Crystallography

For each sample, a crystal was mounted in oil on a glass fibre and fixed in the cold nitrogen stream on an automated CCD diffactometer equipped with Mo Kα radiation ($\lambda = 0.71073$ Å) and a graphite monochromator (10 cm confocal mirrors for **3**); intensity data were measured by thin-slice ω- and θ-scans (**1** and **2**) or thin-sliced ω- and φ-scans (**3**–**10**). Data were processed using the CrysAlis-CCD and -RED,[20] DENZO/SCALEPACK,[21] Bruker APEX II and SAINT[22] programs. The structures were determined by the direct methods routines in the SHELXS[23] or SIR-92[24] programs and refined by full matrix least squares methods, on F^2, using SHELXL.[23] The non-hydrogen atoms were refined with anisotropic thermal parameters. H atoms were included in a riding model. In **1** the imido ligand is disordered across a mirror plane with atoms V(1), O(1), C(1), C(3), N(1), C(5), C(8), C(11), C(26) and C(27) lying on the mirror. In **2** the unique *t*-Bu group is disordered with the methyl groups modelled as split over two sets of positions with major occupancy of 72.5(6)%. The entire CF_3 group at C(3) was disordered over two sets of positions with major occupancy of 80.7(7)%. The second CF_3 group showed some signs of disorder, but was modelled as a single set of positions. In **3** atoms C(6)–C(10) in the imido group were modelled as disordered over two sets of positions with major occupancy of 68.8(8)%. Where disorder was modelled, restraints were applied to both geometry and anisotropic displacement parameters.

Several of the crystals were weakly diffracting, leading to high R_{int} values for **4**, **8** and a low ratio of observed to unique reflections for **5**. In **6**, a short contact between two *tert*-butyl hydrogen atoms was observed: H(19B)···H(35B) 2.03 Å. Neither *tert*-butyl group is disordered, and in both cases the hydrogen atoms are in the local optimal positions. This contact is therefore likely to be a packing artefact.

Acknowledgements

The EPSRC is thanked for financial support. The EPSRC Mass Spectrometry Service (Swansea, UK) and Rapra Smithers Ltd (GPC on polyethylene samples) are thanked for data collection. The EPSRC's National Crystallography Service at the University of Southampton is thanked for the collection of X-ray diffraction data for **3**.

References

1 (*a*) G. J. P. Britovsek, V. C. Gibson and D. F. Wass, *Angew. Chem., Int. Ed.*, 1999, **38**, 428; (*b*) V. C. Gibson and S. Spitzmesser, *Chem. Rev.*, 2003, **103**, 283; (*c*) V. C. Gibson, E. L. Marshall, in *Comprehensive Coordination Chemistry II*, ed. J. A. McCleverty, T. J. Meyer and M. D. Ward, Elsevier, 2004, vol. 9.
2 (*a*) C. Redshaw, D. M. Homden, M. A. Rowen and M. R. J. Elsegood, *Inorg. Chim. Acta.*, 2005, **358**, 4067; (*b*) C. Redshaw, M. A. Rowan, D. M. Homden, M. R. J. Elsegood, T. Yamato and C. Pérez-Casas, *Chem.–Eur. J.*, 2007, **13**, 10129.
3 D. Homden, C. Redshaw, L. Warford, D. L. Hughes, J. A. Wright, S. H. Dale and M. R. J. Elsegood, *Dalton Trans.*, 2009, DOI: 10.1039/b901810g.
4 (*a*) A. Zambelli and G. Allegra, *Macromolecules*, 1980, **13**, 42; (*b*) Y. Doi and T. Keii, *Adv. Polym. Sci.*, 1986, **73–4**, 201; (*c*) S. Gambarotta, *Coord. Chem. Rev.*, 2003, **237**, 229.
5 (*a*) T. Moriuchi, T. Beppu, K. Ishino, M. Nishina and T. Hirao, *Eur. J. Inorg. Chem.*, 2008, 1969; (*b*) T. Moriuchi, K. Ishino, T. Beppu, M. Nishina and T. Hirao, *Inorg. Chem.*, 2008, **47**, 7638.
6 M. Arndt-Rosenau, M. Hoch, J. Sundermeyer, J. Kipke and X. Li, *U. S. Pat.*, 0 130 451, 2003.
7 (*a*) D. D. Devore, J. D. Lichtenhan, F. Takusagawa and E. A. Maatta, *J. Am. Chem. Soc.*, 1987, **109**, 7408; (*b*) M. Lutz, H. Hagen, A. M. M. Schreurs, A. L. Spek and G. Van Koten, *Acta Crystallogr., Sect. C: Cryst. Struct. Commun.*, 1999, **55**, 1636.
8 (*a*) B.-T. Ko and C.-C. Lin, *Macromolecules*, 1999, **32**, 8296; (*b*) D. Takeuchi, T. Nakamura and T. Aida, *Macromolecules*, 2000, **33**, 725; (*c*) H.-L. Chen, B.-T. Ko, B.-H. Huang and C.-C. Lin, *Organometallics*, 2001, **20**, 5076; (*d*) M.-L. Hsueh, B.-H. Huang and C.-C. Lin, *Macromolecules*, 2002, **35**, 5763; (*e*) J. Lewiński, P. Horeglad, E. Tratkiewicz, W. Grzenda, J. Lipkowski and E. Kolodziejczyk, *Macromol. Rapid Commun.*, 2004, **25**, 1939; (*f*) M. Deng, Y. Yao, Q. Shen, Y. Zhang and J. Sun, *Dalton Trans.*, 2004, 944; (*g*) B.-H. Huang, C.-N. Lin, M.-L. Hsueh, T. Athar and C.-C. Lin, *Polymer*, 2006, **47**, 6622.
9 W. A. Nugent and B. L. Haymore, *Coord. Chem. Rev.*, 1980, **31**, 123.
10 D. E. Wigley, *Prog. Inorg. Chem.*, 1994, **42**, 239.
11 P. J. Toscano, E. J. Schermerhorn, C. Dettelbacher, D. Macherone and J. Zubieta, *J. Chem. Soc., Chem. Commun.*, 1991, 933.
12 D. Maity, A. Ray, W. S. Sheldrick, H. Mayer Figge, B. Bandyopadhyay and M. Ali, *Inorg. Chim. Acta*, 2006, **359**, 3197.
13 C. Redshaw, M. A. Rowan, L. Warford, D. M. Homden, A. Arbaoui, M. R. J. Elsegood, S. H. Dale, T. Yamato, C. P. Casas, S. Matsui and S. Matsuura, *Chem.–Eur. J.*, 2007, **13**, 1090.
14 A. W. Addison, T. N. Rao, J. Reedijk, J. Van Rijn and G. C. Verschoor, *J. Chem. Soc., Dalton Trans.*, 1984, 1349.
15 See for example: C. Redshaw and S. M. Humphrey, *Polyhedron*, 2006, **25**, 1946, and references therein.

16 J.-K. F. Buijink, A. Meetsma, J. H. Teuben, H. Kooijman and A. L. Spek, *J. Organomet. Chem.*, 1995, **497**, 161.
17 (*a*) C. Redshaw, M. A. Rowan, D. M. Homden, S. H. Dale, M. R. J. Elsegood, S. Matsui and S. Matsuura, *Chem. Commun.*, 2006, 3329; (*b*) D. M. Homden, C. Redshaw and D. L. Hughes, *Inorg. Chem.*, 2007, **46**, 10827; (*c*) D. Homden, C. Redshaw, J. A. Wright, D. L. Hughes and M. R. J. Elsegood, *Inorg. Chem.*, 2008, **47**, 5799.
18 (*a*) K. Nomura, A. Sagara and Y. Imanishi, *Chem. Lett.*, 2001, 38; (*b*) W. Wang, J. Yamada, M. Fujiki and K. Nomura, *Catal. Commun.*, 2003, **4**, 159; (*c*) Y. Nakayama, H. Bando, Y. Sonobe, Y. Suzuki and T. Fujita, *Chem. Lett.*, 2003, **32**, 766; (*d*) Y. Nakayama, H. Bando, Y. Sonobe and T. Fujita, *J. Mol. Catal. A*, 2004, **213**, 141; (*e*) Y. Nakayama, H. Bando, Y. Sonobe and T. Fujita, *Bull. Chem. Soc. Jpn.*, 2004, **77**, 617; (*f*) A. K. Tomov, V. C. Gibson, D. Zaher, M. R. J. Elsegood and S. H. Dale, *Chem. Commun.*, 2004, 1956; (*g*) W. Wang and K. Nomura, *Macromolecules*, 2005, **38**, 5905; (*h*) L.-M. Tang, J.-Q. Wu, Y.-Q. Duan, L. Pan, Y.-G. Li and Y.-S. Li, *J. Polym. Sci., A*, 2008, **46**, 2038; (*i*) J. Q. Wu, L. Pan, N. H. Hu and Y. S. Li, *Organometallics*, 2008, **27**, 3840.
19 M. Möller, R. Kånge and J. L. Hedrick, *J. Polym. Sci., A*, 2000, **38**, 2067.
20 *CrysAlis-CCD and -RED*, Oxford Diffraction Ltd., Abingdon, UK, 2005.
21 Z. Otwinowski, W. Minor, Processing of X-ray diffraction data collected in the oscillation mode, in *Methods in Enzymology*, ed. C. W. Carter, Jr. and R. M. Sweet, Academic Press, New York, 1997, vol. 276, pp. 307–326.
22 *APEX II and SAINT software for CCD diffractometers*, Bruker AXS Inc, Madison, WI, USA, 2006.
23 G. M. Sheldrick, *Acta Crystallogr., Sect. A: Fundam. Crystallogr.*, 2008, **64**, 112.
24 A. Altomare, G. Cascarano, C. Giacovazzo and A. Guagliadi, *J. Appl. Crystallogr.*, 1993, **26**, 343.

